

## CHAPTER V

### RESULTS

#### 5.1. Spectral Signatures Analysis and Spectral Signatures of Minerals, Rocks

Signature differences were studied and compared at different multispectral wavelengths and between ASTER and Landsat TM (Thematic Mapper) images. Surface temperature and brightness are the physical properties accessible in the thermal infra-red to high-frequency range. These parameters are affected by the chemical nature of rocks and their rock types. Thermal inertia, the conventional term used in remote sensing for the heat capacity of rocks, is another physical property which facilitates the spatial interpretation of spectral signatures.

Spectral signatures are useful for distinguishing minerals and certain rocks of homogeneous composition. Absolute intensity of reflectance which varies with wavelength and gives rise to variations in amplitude of signal. A multispectral satellite image is composed of several images which have been recorded simultaneously over the exact same area. Each image shows the surface reflection of sunlight within certain wavelengths called channels. The surface of every object has its own spectral signature. The surface of the water reflects sunlight in specific amounts in channel 1, channel, 2, 3...channel 7 (landsat TM) or channel 14 (ASTER)...etc. The spectral signatures of different area types are to be measured by MultiSpec software (See figure- 5.1).

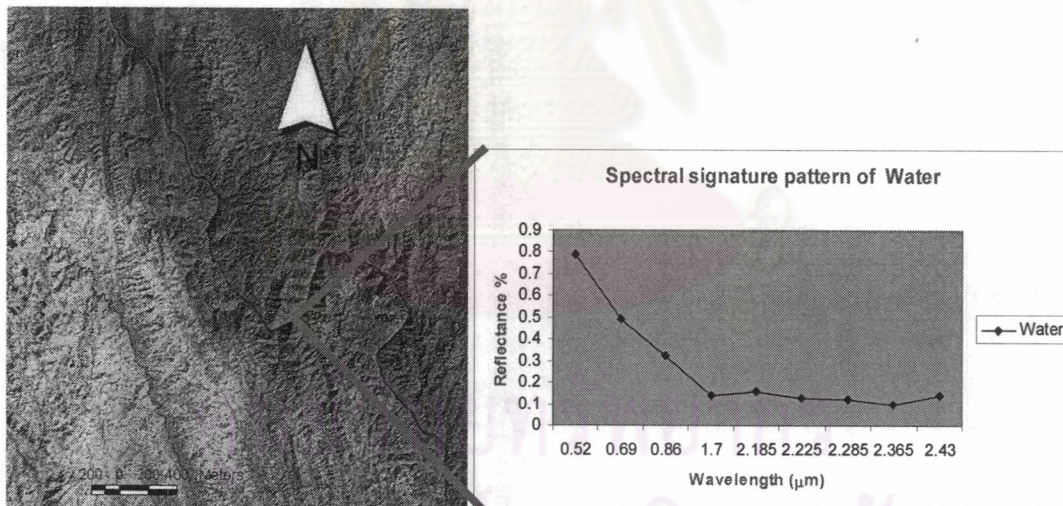


Figure-5.1. Graph window showing the spectral signature pattern using by the Multispec Software.

In the Selection Graph window channels 1, 2,3...14 are seen on the x-axis. The pixel values are seen on the y-axis. The graphs show the pixel values of the selected area or rock has in channels 1, 2,3 ,... channel 7 (landsat TM) or channel 14 (ASTER) image respectively. Where channel 1 to 3 will be the VNIR. Channel 4,5,..9 will be SWIR and channel 10,11,..14 will be TIR value .Note that the y-axis in the Graph

window changes with every measuring, so be careful when reading the average pixel values.

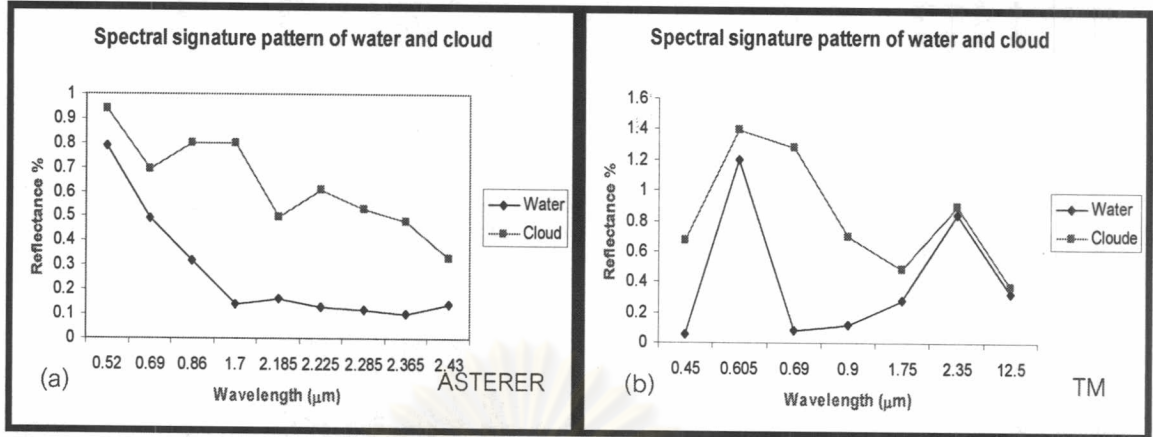
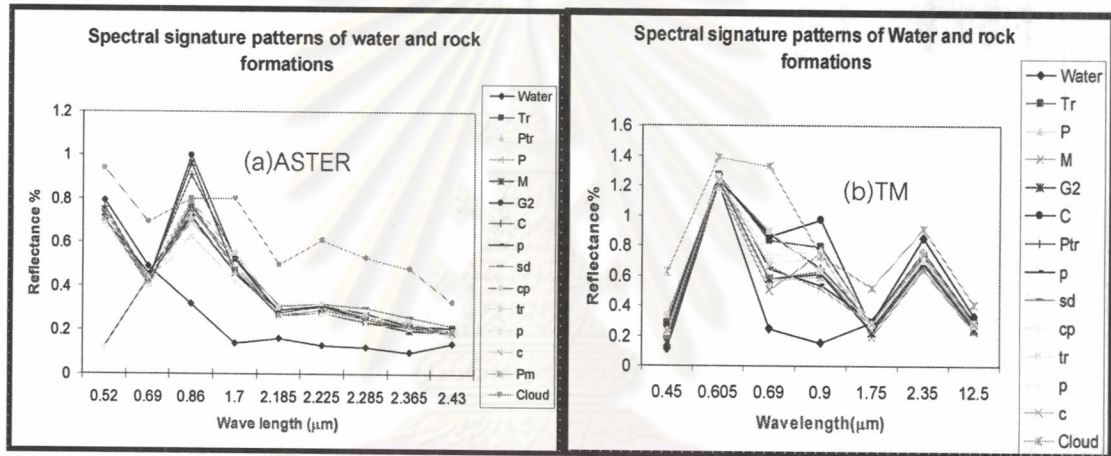


Figure-5.2. Graph showing the spectral signature pattern of water and cloud .



Figure–5.3. Graph showing the spectral signature pattern of water and rock formations(a) ASTER result and (b) TM result.

## 5.2. Supervised Classification

The spectral information represented by the digital numbers in one or more spectral bands, and attempts to classify each individual pixel based on this spectral information. This type of classification is termed spectral pattern recognition. We need to distinguish between information classes and spectral classes. Information classes are those categories of interest that the analyst is actually trying to identify in the imagery such as different geologic units or rock types and water. Spectral classes are groups of pixels that are uniform (or near-similar) with respect to their brightness values in the different spectral data. The objective is to match the spectral classes in the data to the information classes of interest.

Using the rock formation, spectral sub-classes may be due to variations in mineral composition, age, species, and density. It is the analyst's job to decide on the utility of the different spectral classes and their correspondence to useful information classes.

### 5.2.1. Scatter Plots

Scatter plots are the most commonly used methods to project high dimensional data to a 2D space. In this method,  $n*(n-1)/2$  pair-wise parallel projections are generated, where  $n$  is the number of dimensionality. Each scatter plot gives the analyst a general impression regarding relationships within the data between pairs of dimensions. Figure 5.4 shows a 2D scatter plot of classification with band 4 and 5. The pixels within one class cluster together and can be considered as a pattern. Thus the characteristics of classes can be interpreted by "pattern recognition" based on the statistic approach. For example, the separability analysis calculates the distances between two different classes for various band combinations. Then the bands with large distance can be selected as useful features.

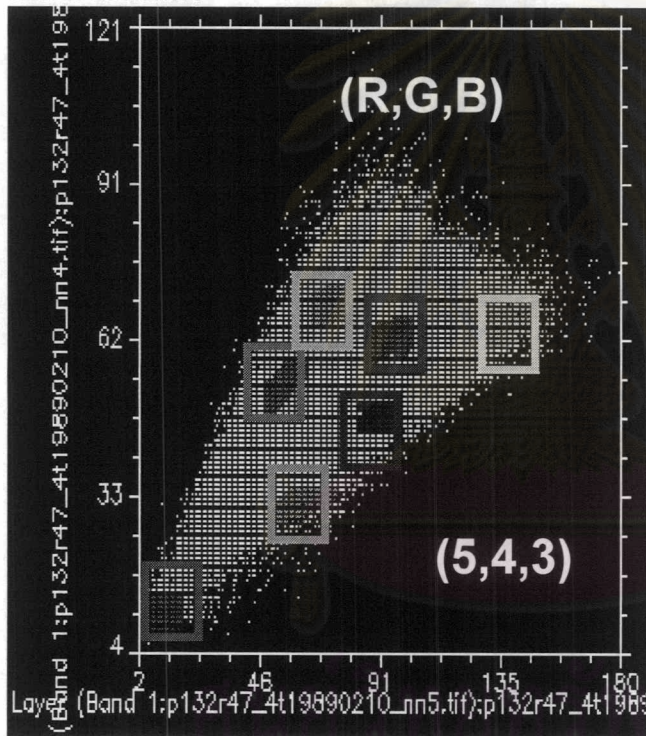


Fig-5.4. 2D scatter plotting of Landsat TM (R,G,B); (5,4,3)

This image shows a scatter plot of the area using TM bands 4 and 5. Signatures created from the supervised classification are outlined on this image. The AREA was used to view the statistics concerning each rock formations, and group. This information will later be compared to data generated from the unsupervised classification example.

### 5.2.2. Maximum Likelihood Classification

This attempt was made to classify the various rock units use in ENVI .4 and image processing using supervised classification techniques. In supervised classification, spectral signatures are developed from specified locations in the image. These specified locations are given the generic name 'training sites' and are defined by the 2D scatter plotting method. Generally a vector layer is digitized over the raster scene. The vector layer consists of various polygons overlaying different rock formation types.

The AREA module in the study area was used to view the statistics concerning each lithologic group. This information will later be compared to data generated from the Landsat TM and ASTER data set.

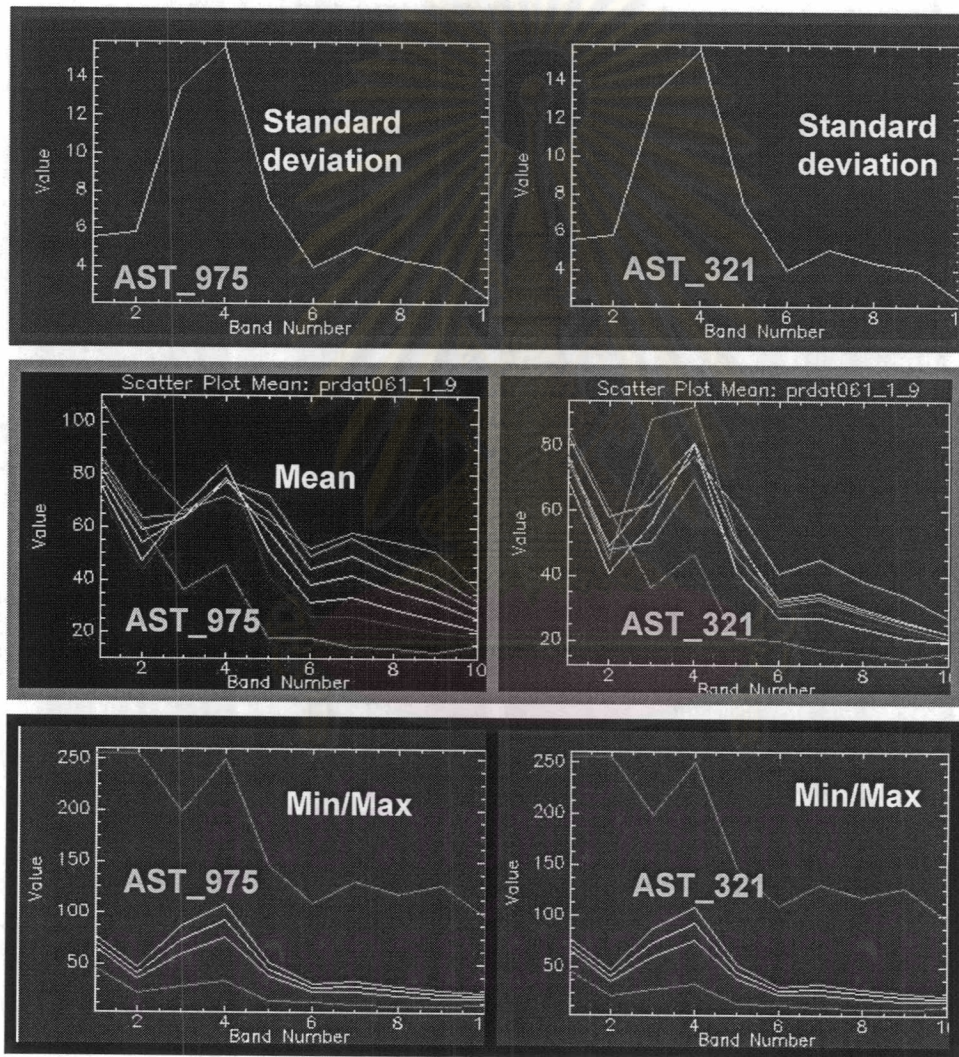


Figure-5.5. Statistics report of ASTER (R,G,B); (9,7, 5) and (3,2,1)

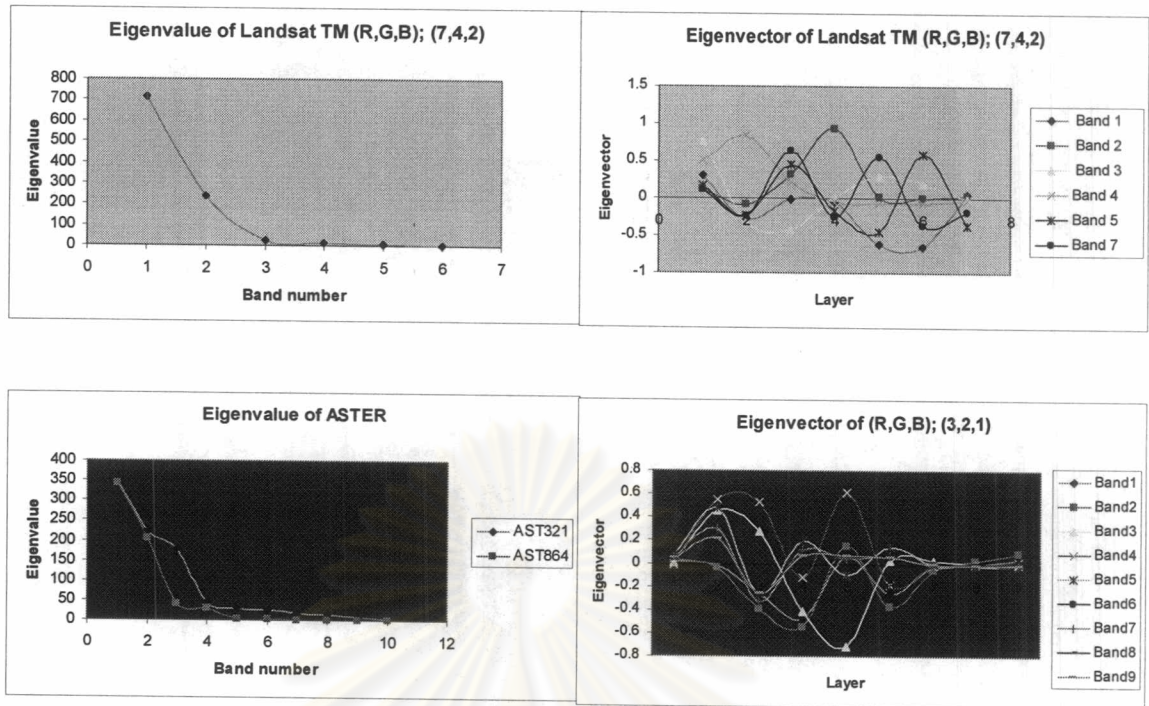


Figure -5.6. Results of eigenvalue and Eigenvector (a) TM and (b) ASTER.

Band	Min	Max	Mean	Stdev	Eigenvalue
1	46	255	72	5.516390	4775.83
2	22	255	41	5.819751	348.36
3B	28	199	74	13.465797	146.83
3N	33	251	92	15.588628	67.67
4	14	146	45	7.490231	35.98
5	13	109	27	3.996186	22.43
6	11	130	28	5.070114	19.30
7	10	118	24	4.376785	15.09
8	9	127	21	3.997393	9.88
9	12	98	19	2.389600	3.86

Table-5.1.(a) Statistics report of ASTER (R,G,B); (9,7, 5)

Band	Min	Max	Mean	Stdev	Eigenvalue
1	1.000000	91.000	28.3794	10.710511	809.148434
2	117.0000	146.000	129.63314	4.449776	102.203484
3	2.0000	173.000	73.398075	23.279031	26.187318
4	4.0000	121.000	55.719706	13.339452	6.705614
5	14.0000	85.000	31.439388	7.259128	4.003247
6	18.0000	65.000	28.535006	3.573378	2.777190
7	61.0000	137.000	77.043663	5.671835	0.978222

Table-5.1(b) Accuracy assessment of the classification Result of Landsat TM (R,G,B);  
(7,4,2)

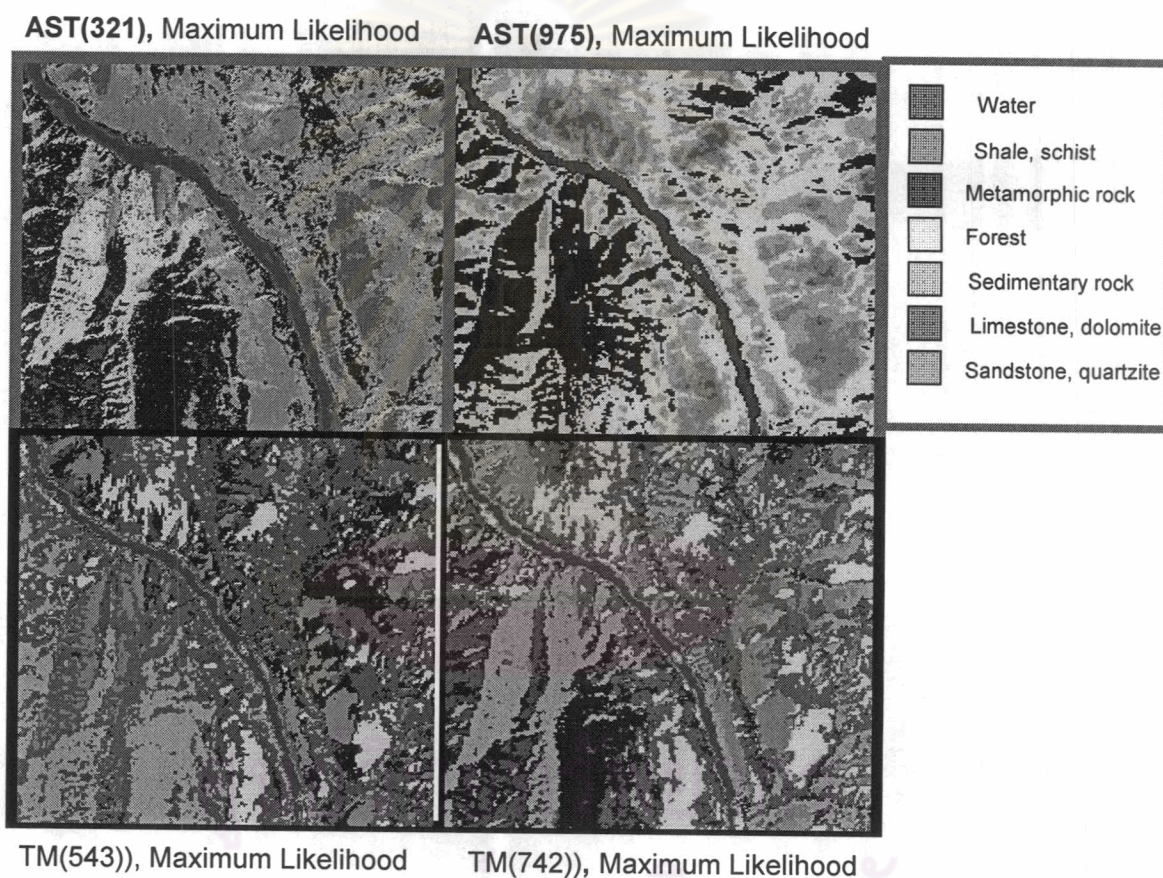


Figure-5.7. Result of Maximum-Likelihood classification

Cover Type	Number Pixels	Area (Ha)
Water	3218	62.055
Shale, schist	103	176.085
Metamorphic rock	5910	340.695
Forest	10119	539.640
Sedimentary rock	5862	349.830
Limestone, dolomite	266	20.250
Sandstone, quartzite	34	1.530

Overall Accuracy =  $(25512/160000) = 15.9450\%$

Kappa Coefficient = 0.0339

Table-5.2. Summary statistics on extent of cover types in a scene

At this area, the image is difficult to interpret. Decisions need to be made concerning which rock types each category falls within. To make these decisions, other materials and knowledge of the area are useful. Ground truthing what is seen in the digital image with what was actually present. The image was recorded makes this task more efficient and more accurate. If this knowledge is not available, scientific reasoning may be used to group the various rocks together into rock formation. Five classes were identified from the original 12 rock formations and are shown in the image (see figure-5.7 show the results of the object-oriented and pixel based maximum likelihood classification approaches, respectively.).

This scene was part of a 1984 study of how accurately we can identify rock units using Landsat TM data from arid (vegetation, forest) terrains. First we present a Maximum Likelihood Supervised classification of the scene Landsat TM on 10 February, 1989 and ASTER on 19 May, 2000, made on the digital image processing system. Its classification accuracy is an estimated 16%; that is, the rock units or formations are correctly identified over at least that percentage of surface exposures (sources of error: soil cover and similar lithologies). This is high in view of shadow and slope effects, soil cover, and other variables.

The above classification applies a different set of training sites and, unlike the one above, includes VNIR Band 2, NIR band 7 and 4 of Landsat TM and SWIR band 9, 7, and band 5 of ASTER. The formations are exceptionally distinct. Red was assigned to water. The large section of blue occupying the metamorphic rock formation corresponds to strongly weathered slope wash along steep slopes.

### 5.3. Classification Accuracy Assessment

The accuracy of the final product depends on the quality of the input data (rubbish in, rubbish out) and on the accuracy of all processing that is performed on the data. Therefore, every step in the workflow will be discussed in order to get some insight in the final accuracy of the end product.

Ground truth is necessary to assess the accuracy of a classification. This ground truth is in addition to the ground truth used in the actual classification process. Sometimes Classification Error Matrix is called Confusion Matrix using by ENVI.4. Compares the relationship between known reference data (ground truth) and the corresponding results of the classification.

Alternatively, an error matrix generated from other sources may also be provided. The elements of the error matrix are used to derive a number of accuracy measures, which have been divided into Percent correct measures and Kappa coefficient.

An average accuracy of 17.09% and an overall accuracy of 15.95% was achieved with a Kappa coefficient of 0.0339. The average accuracy is the average of the accuracies for each class, and the overall accuracy is a similar average with the accuracy of each class weighted by the proportion of test samples for that class in the total training or testing sets. Thus, the overall accuracy is a more accurate estimate of accuracy.

### 5.4. Univariate and Multivariate Statistics

The results of the univariate analysis are as shown in Table-5.3(a) and (b). They show that band 2 has the smallest variance due to its low contrast and band 4 has the largest variance due to the large differences in the spectral response in this band, of the various materials contained in the TM image. Also band 9 has the smallest variance and band 3 has the largest variance due to the large differences in the spectral response in this band, of the various materials contained in the ASTER image.

ศูนย์วิทยทรัพยากร  
จุฬาลงกรณ์มหาวิทยาลัย



Band Number	TM 1	TM 2	TM 3	TM 4	TM 5	TM 6	TM 7
Mean per band	28.13	129.63	73.40	55.72	31.44	28.54	77.04
Stdev per band	10.71	4.45	23.28	13.34	7.26	3.57	5.67
Variance	88.86	21.03	450.14	343.80	40.46	12.40	36.15

Table-5.3.(a). Univariate analysis on the 7 bands of Landsat TM image.

Band Number	AST1	AST2	AST3	AST4	AST5	AST6	AST7	AST8	AST9
Mean per band	76.54	49.35	65.13	49.86	32.17	34.02	29.44	25.62	22.18
Stdev per band	5.36	7.48	9.00	10.34	6.43	8.40	6.94	6.23	3.59
Covariance	28.68	55.96	81.08	129.68	106.96	41.36	70.49	48.18	38.76

Table-5.3(b). Univariate analysis on the 9 bands of ASTER image.

The correlation matrix (see Table-5.4 (a) and (b) ) represents the multivariate statistics . There indicate that bands TM-1, TM-2, and TM-5 are highly correlated. Therefore their information is redundant. The lowest correlation is obtained for bands TM-4 and TM-7 (1.89%) making them the most important in establishing differences on the basis of spectral information. In the ASTER image , band 1 , band 2 and band 9, and band 7 are highly correlated. The lowest correlation is obtained for bands 2 and 4 (0.43%) making them the most important in establishing differences on the basis of spectral information.

Band	TM 1	TM 2	TM 3	TM 4	TM 5	TM 6	TM 7
TM 1	1	0.670999	0.934678	0.297491	0.878254	0.845434	0.736113
TM 2	0.670999	1	0.656057	0.279218	0.668277	0.65954	0.608764
TM 3	0.934678	0.656057	1	0.532287	0.770213	0.801208	0.629011
TM 4	0.297491	0.279218	0.532287	1	0.115228	0.301022	-0.00189
TM 5	0.878254	0.668277	0.770213	0.115228	1	0.922276	0.867201
TM 6	0.845434	0.65954	0.801208	0.301022	0.922276	1	0.863414
TM 7	0.736113	0.608764	0.629011	-0.00189	0.867201	0.863414	1

Table-5.4.(a).Correlation matrix of Landsat TM image for the study area.

(b).Correlation matrix of ASTER image for the study area.

Band	AST 1	AST 2	AST 3	AST 4	AST 5	AST 6	AST 7	AST 8	AST 9
AST1	1	0.91	-0.13	-0.37	0.31	0.48	0.47	0.48	0.50
AST2	0.912	1	-0.23	-0.43	0.36	0.55	0.53	0.54	0.56
AST3	-0.13	-0.23	1	0.68	0.38	0.15	0.17	0.15	0.14
AST4	-0.37	-0.43	0.68	1	0.20	-0.02	0.01	-0.01	-0.02
AST5	0.31	0.36	0.38	0.20	1	0.94	0.95	0.94	0.93
AST6	0.48	0.55	0.15	-0.02	0.94	1	0.99	0.98	0.98
AST7	0.47	0.53	0.17	0.01	0.95	0.99	1	0.98	0.98
AST8	0.48	0.54	0.15	-0.01	0.94	0.98	0.98	1	0.99
AST9	0.50	0.56	0.14	-0.02	0.93	0.98	0.98	0.99	1

### 5.5. Low Pass Filters

Digital image processing technique was performed to extract rock units and forest cover categories from fused images in different phases. Image pre-processing was carried out including image rectification. Image rectification of all three images were performed using first order polynomial equation. Image to map and image to image registrations were applied to images in order to prepare them for an accurate fusion application.

Low pass filtering preserves the low frequency components of an image, which smooths it. ENVI's default low pass filter contains the same weights in each kernel element, replacing the center pixel value with an average of the surrounding values. The default kernel size is 3 x 3 , and 5 x 5 .

$$\text{Mask Template} = \begin{matrix} c_1 & c_2 & c_3 \\ c_4 & c_5 & c_6 \\ c_7 & c_8 & c_9 \end{matrix}$$

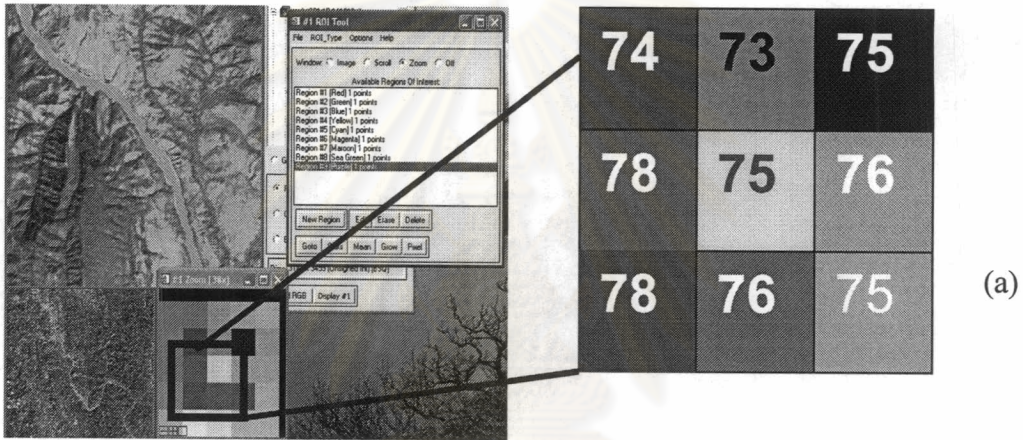
$$BV_5 = \Sigma \begin{matrix} c_1 \times BV_1 & c_2 \times BV_2 & c_3 \times BV_3 \\ c_4 \times BV_4 & c_5 \times BV_5 & c_6 \times BV_6 \\ c_7 \times BV_7 & c_8 \times BV_8 & c_9 \times BV_9 \end{matrix}$$

$$\Sigma = \dots\text{new pixel value}$$

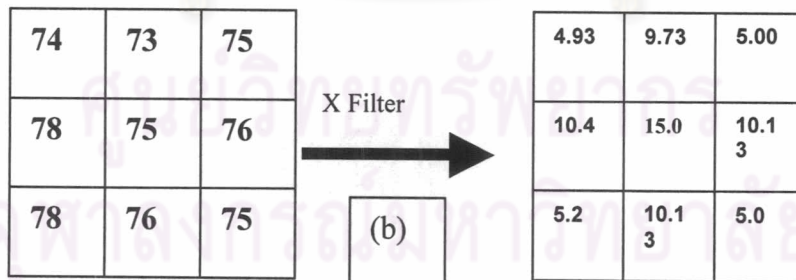
$$\text{Mask Template} = \begin{matrix} c_1 & c_2 & c_3 \\ c_4 & c_5 & c_6 \\ c_7 & c_8 & c_9 \end{matrix}$$

$$BV_5 = \Sigma \begin{matrix} c_1 \times BV_1 & c_2 \times BV_2 & c_3 \times BV_3 \\ c_4 \times BV_4 & c_5 \times BV_5 & c_6 \times BV_6 \\ c_7 \times BV_7 & c_8 \times BV_8 & c_9 \times BV_9 \end{matrix}$$

$\Sigma = \dots$ new pixel value



$$\text{Low-Pass; } c_i = \begin{matrix} 1/15 & 2/15 & 1/15 \\ 2/15 & 3/15 & 2/15 \\ 1/15 & 2/15 & 1/15 \end{matrix}$$



$\Sigma = 75.52$ , new pixel value

Figure-5.8(a) and (b) Image showing pixel values of the 3 x 3 window

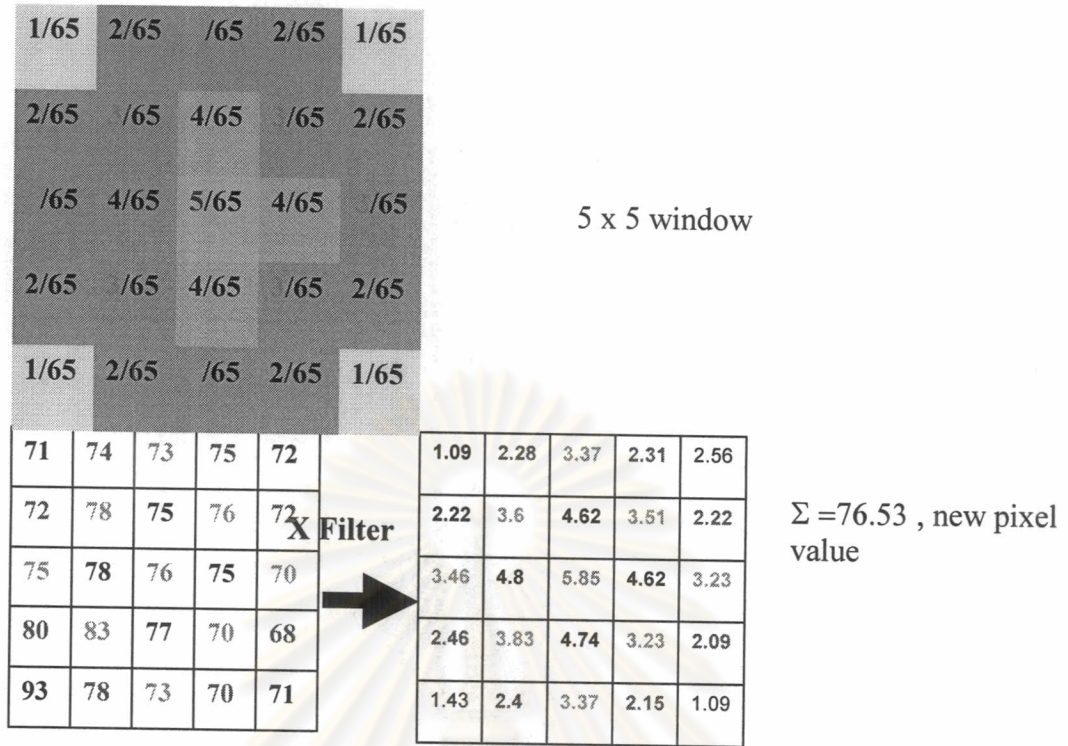


Figure-5.9. Image showing the 5 x 5 window.

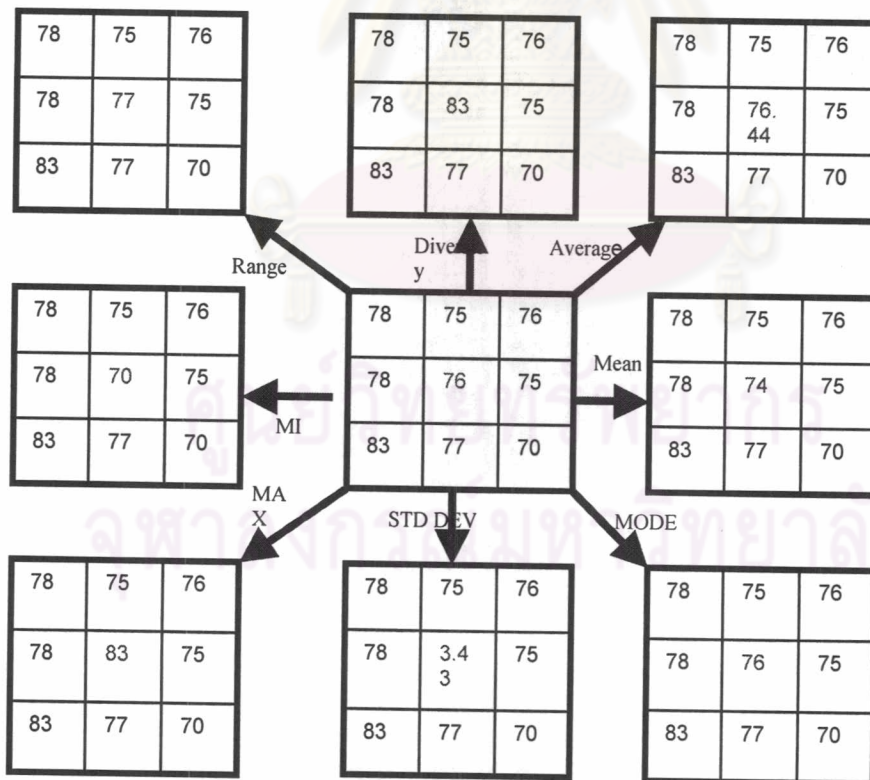


Figure- 5.10. Window operation for spatial filtering.

The value for the cell at the centre of the window is computed as a simple arithmetic average of the values of the other cells (see figure-5.10 ). Mean can be computed by multiplying the cell values in the window by the  $n \times m$  values in the filter. Mean of  $3 \times 3$  and  $5 \times 5$  for the window center can be computed by multiplying each cell value by a weight of  $1/9$ ,  $1/25$  and adding all results. That can be replaced by the mode, which is the most common value.

The low-pass filter has the effect of removing extremes from the data, that will be producing a smoother image (see figure- 5.11 ). Diversity of the four directional axes within the window are alternative options. The diversity is useful operations for indicating the local complexity of the spatial pattern.

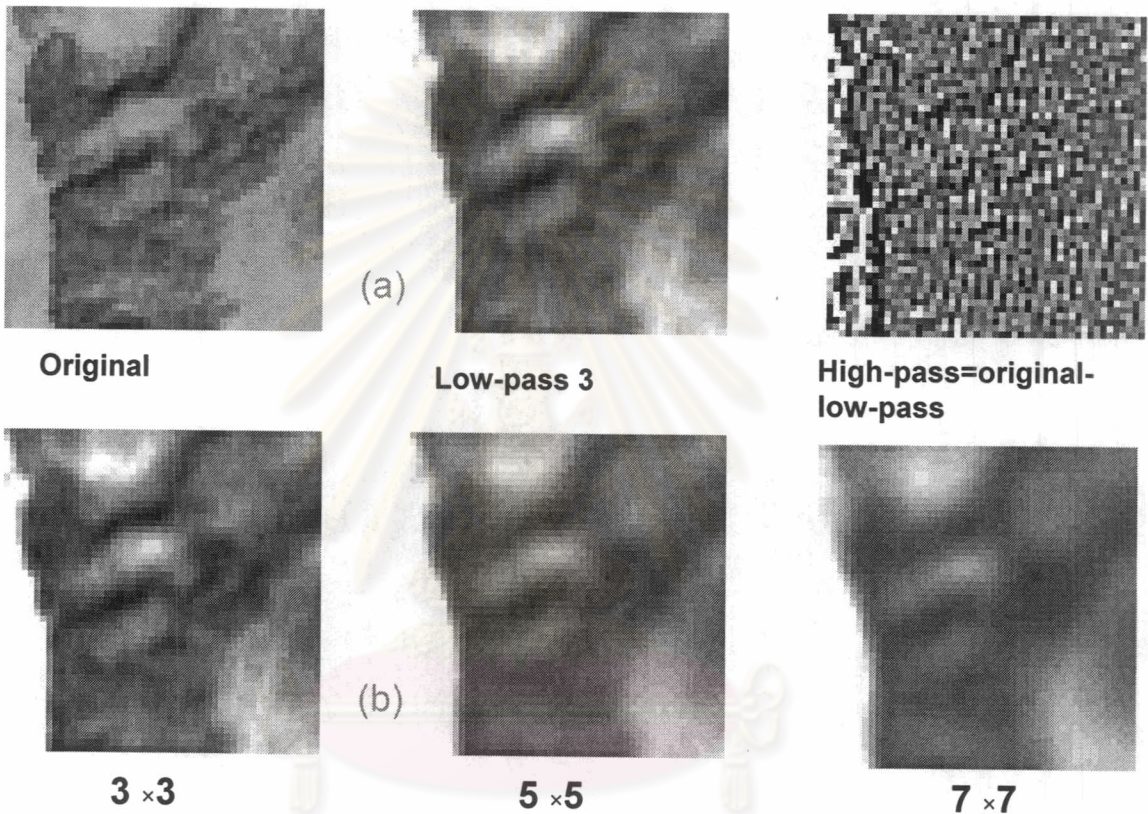


Figure- 5.11. (a)Smoothing a surface with a low-pass filter and (b) the effect of increasing window size on smoothing.

### 5.6. Geological Mapping

A geological map is the result of integration of ground observations and measurements made on outcrops that are often discontinuous. It is a complex geological document which combines the chronology, geometry and geomorphology on a topographic and drainage base. It is the final document resulting from interpretation of observed facts and hence is greatly influenced by the concept of mapping and the

structural hypotheses adopted. Some of the factors that strongly affect the results of mapping are:

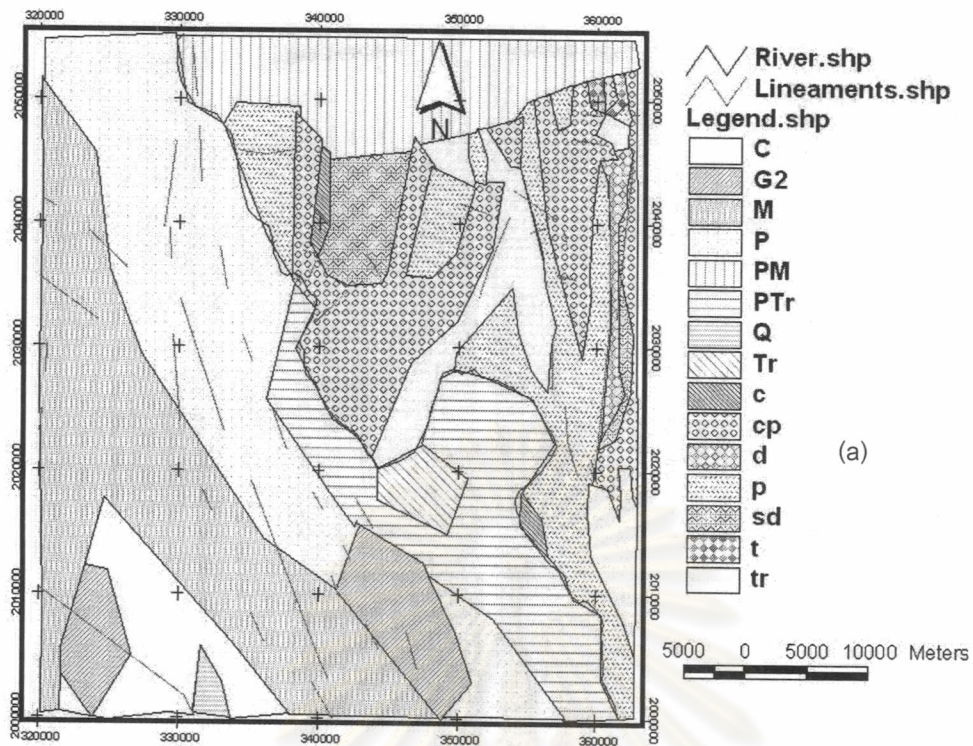
- a. Stratigraphy, which predominantly influenced, i.e., the effect of major stratigraphic boundaries on the (chemical nature) composition of rocks.
- b. Lithology: certain maps highlight differences in the nature of rocks while preserving the stratigraphic connotation.

The efficiency of remote-sensing interpretation, which is very sensitive to the relief. That is enhanced when geomorphology is fully taken into account. Lineament distribution and its general orientation are shown in Figure-6.1. Major lineament trend can be summarized as N-S, NW-SE under considering exaggeration due to imaging orientation. N-S structure is the most dominant orientation.

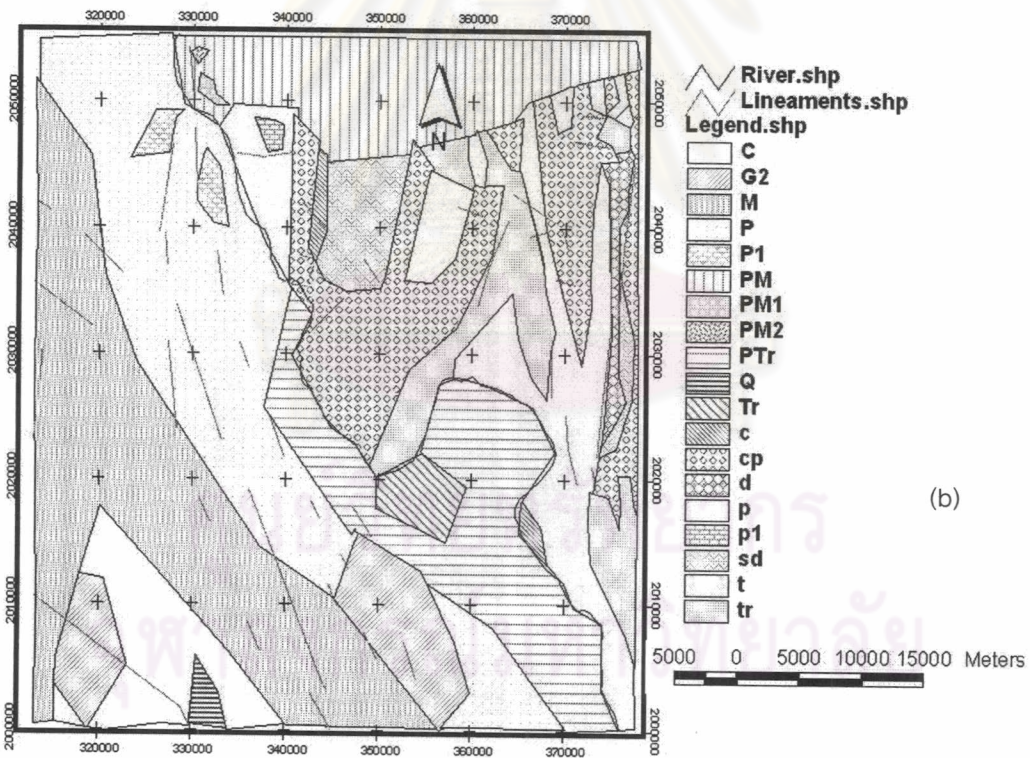
The geological map of study area was compiled from geological hardcopy maps at 1:2000,000 scale and 1:500,000 scale published in 1981, 1983 by (Geology of Burma and Mineral resource of Thailand ). The map covers the area from longitude 97 degree to 98 degree East . The extent of the digitally compiled map is 1: 250,000 scale geological hardcopy map of study area (See figure-5.12 ). The map is mainly composed of geological body layer (outcrop polygon). Geological bodies were classified according to their generic type to sedimentary, metamorphic, igneous rock. Each class was divided into many rock types depending on their lithological characteristic and age. Each polygon was assigned code value, all records of code field contain a 2 digit string. Each code indicates the type of rocks, based on lithology and age.

Function as a visual base on this geologic map is drawn either directly or on a digitizing overlay. With the Landsat TM and ASTER images, we now can extend this is the advantage of coverage area allows them to examine in physical scene as the geological of earth on a regional basis. The ability to analyze multispectral bands quantitatively in spectral signature patterns them to apply Multispec, ENVI 4 processing routines to image classification and enhance certain compositional properties of earth materials as lithology. The capability of merging different types of remote sensing products such as reflectance or combining these with topographic elevation data, drainage patterns and with other kinds of information bases such as geological maps; structure lineaments enables new solutions to determining interrelations among various natural properties of earth phenomena.

ศูนย์วิทยทรัพยากร  
จุฬาลงกรณ์มหาวิทยาลัย


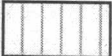


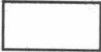
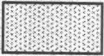
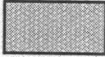



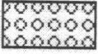
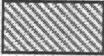
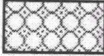



(a)



(b)

Fig-5.12. Geological map of study area ( (a). overlaying map and , (b) new map)

<u>Symbol</u>	<u>Lithology</u>	<u>Age</u>
	Shale, bone beds, evaporates, limestones	Triassic
	Undifferentiated sediments of Eastern Burma	Paleozoic- Mesozoic
	Limestone, dolomite	Paleozoic-Triassic
	Slate, Phyllite, quartzite, and subordinate schists	Paleozoic, undifferentiated
	Quartzites, greywacke and conglomerates	Carboniferous
	Gneiss and Hybrid rocks	Metamorphics, undifferentiated
	Granite, diorite, and their medium and fine grained equivalents	Mesozoic and Cenozoic
	Sandstone, shale oil shale, lignite, limestone, and locally rare conlomerate	Tertiary
	Marine: sandstone, tuffaceous sandstone, limestone, and conlomerate	Middle Triassic
	Massive limestone, dolomite , sandstone , siltstone and shale	Middle permian
	Sandstone, shale and chert	Upper Carboniferous to lower Permian
	Conglomerate , sandstone, shale, slate , chert beds, and limestone	Middle Carboniferous
	Shale, chert , limestone and sandstone	Devonian
	Quartzite, phyllite ,schist, sandstone, shale, and tuff	Silurian to Devonian



We can do new map on how Landsat Thematic Mapper TM data and ASTER for this region is manipulated to identify different rock types, map them overlaying area using supervised classification, and correlate their spatial patterns with independent information on their structural arrangement. New geologic map is also stratigraphic map, that is, we extended to record the location and identities of sequences of rock types according to their relative ages. The fundamental rock unit is the formation (abbreviated as Fm or fm), defined simply as a distinct mappable set of rocks (if sedimentary, then usually layered) that has a specific geographic distribution. A formation typically is characterized by one or two dominant types of rock materials, so we can extended one or two of their rock units.

The spectral response of each pixel in a Landsat TM image and ASTER in study area, due to the limited spatial resolution, be considered as a mixture of spectral signatures from forest, water, limestone, sedimentary rocks and metamorphic rock. As illustrated in figure 12(b) a new map, a new 3 endmembers were extracted from the TM and ASTER image such as sedimentary and metamorphic rocks, limestone, shale, and schists. These endmembers were all significantly different from each other, thus could be used with confidence for classification. All endmember was selected in the TM image where it was selected in their location and extended in database. Results of new mapping effort is summarized from different scale geological map, environment variables (geographic region, elevation, slope-aspect), supervised classification and political boundary.



ศูนย์วิทยทรัพยากร  
จุฬาลงกรณ์มหาวิทยาลัย